Disruption Mitigation Experiments in the JT-60U Tokamak

M. Bakhtiari 1), Y. Kawano 1), H. Tamai 1), G.J. Kramer 2), A. Isayama 1), Y. Kamiya 1), R. Yoshino 1), Y. Miura 1), Y. Kusama 1), H. Takenaga 1), T. Nakano 1), H. Kubo 1), Y. Nishida 3), JT-60 Team 1)

1) Naka Fusion Research Establishment, Japan Atomic Energy Research Institute, Japan
2) Princeton Plasma Physics Laboratory, USA.
3) Utsunomiya University, Japan

e-mail contact of main author: bakhtiar@fusion.naka.jaeri.go.jp

Abstract. Experiments in the JT-60U tokamak have shown that disruption deleterious effects on plasma facing components of a tokamak reactor can be greatly reduced or avoided by simultaneous puffing of small amounts of high-Z noble gases, particularly, krypton and large amounts of hydrogen gas. A high electron density caused by the intense hydrogen gas puffing amplified the radiation of High-Z atoms. In turn the stored energy was radiated and plasma was terminated quickly. The high electron density and high effective charge made by high-Z species prevents runaway electron generation. It was also found that injecting neon ice pellets during the post-disruption runaway plasma can enhance the runaway electron losses.

1. Introduction

Disruptions, a sudden lose of the thermal energy and quenching the plasma current, are a consequence of violating operational limits in tokamaks. Disruptions may have some critical effects on plasma facing components if they occur: 1) high heat fluxes to the divertor plates and wall, 2) electromagnetic forces by induction currents during the current quench and mechanical stresses due to halo currents, and 3) relativistic runaway electrons that will ultimately be lost onto the wall with possible damaging effects. Future devices are expected to be operated well within a safe disruption-free regime but for unforeseen events such as control system failures the fusion device has to be switched off safely before a disruption can damage the machine.

Advancing disruption avoidance through active plasma control is of a high priority but in the case of a control system failure or other abnormal events, techniques must be available to mitigate or avoid the disruption deleterious effects. This issue has been examined by means of enhancing the radiation power of the plasma in order to remove the energy of the plasma by cooling it down. The plasma current decays quickly as the plasma resistivity of a cold plasma is high. Normally, the radiation power is enhanced by intentionally pushing the density or impurity contamination well beyond the radiation limits [1-3].

Available disruption mitigation techniques have to be advanced yet: killer pellet injection [1] deposits the species locally and sometimes is followed by runaway electron generation. High pressure gas injection [2] introduces very intense radiation power deposition on the walls and may also induce large electromagnetic forces due to induction currents. We have explored a novel technique with less or no runaway electron generation, controllable radiation powers and current quench rates by injecting a mixture of impurities and hydrogen gas. In these disruption mitigation experiments we have used gas puffing with a mixture of small amounts of high-Z noble gases: argon (Ar^{18}), krypton (Kr^{36}), and xenon (Xe^{54}) and large amounts of hydrogen. The potential of each of these noble gases in runaway electron generation and heat fluxes to the divertor plates has been compared.

In cases where disruption avoidance fails for some reason, runaway electrons can be generated. In such situations, runaway electrons must be managed safely. For this purpose, a slow termination of a runaway current with keeping the appropriate plasma shape and position [5] is beneficial. But, when this slow termination is not available because of a fast growth of vertical disruption event or plasma control system failure, a quick mitigation of the runaway electrons is essential. It is known that runway electrons are promptly lost due to large MHD activity when surface safety factor, q_s, becomes small as 2 or 3 [6],[7]. However, pulsive and localized heat load to the first wall by runaway electrons [7] is still a concern. Here, we investigate another approach to mitigate runaway electrons by use of external actuators with good controllability. When the disruption has already occurred and has led to runaway electron generation, we have studied the possibility of mitigating the damaging effects of runaway electrons by impurity pellet (neon pellet) injection.

2. Experiments

The disruption mitigation experiments we have done in JT-60U are classified in two main categories. The first set was carried out in order to terminate stable discharges with reducing the heat flux to the divertor plates and avoiding runaway electron generation during the thermal and current quenches using gas puffing (section 2.1). The second set was carried out in order to study the possibility of terminating the runaway current of disrupted plasmas using multiple killer pellet injection (section 2.2).

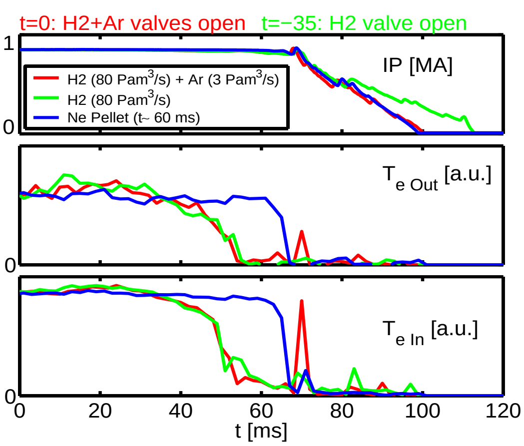

Figure 1.Time traces of plasma current and electron temperature at two different radial positions for discharges terminated with mixture gas puffing, hydrogen gas puffing, and neon killer pellet injection. During the gas puffing electron temperature slowly decreases from outer regions whilst this is done very quickly with a killer pellet. The resulted current quenches with killer pellet and mixture gas look similar for these shots. Only for this set of experiments Bt~ 1.8 T.

Ohmically heated plasmas with I_p=0.85 MA, B_t=1~3.85 T, and $\overline{n}_e \sim 1\times10^{19}$ m^{-3}were used as target plasmas. The gas puff rate is expressed in a unit of Pa m^3/s which corresponds to 2.4×10^{20} atoms at room temperature.

2.1. Plasma termination experiments

In earlier studies of disruption mitigation experiments it was shown that tokamak discharges can be terminated quickly by injecting a killer pellet [1]. However, this method usually is followed by a runaway current. Recently it has been shown that the injection of a mixture of argon and a large amount of hydrogen gas into a discharge can terminate the discharge quickly without runaway electron generation [3]. However, these two different techniques have not been examined under the same experimental conditions yet. In order to make such a comparison we carried out three different plasma termination experiments using killer pellet (neon ice pellet) injection, mixture gas puffing, and hydrogen gas puffing. The results are shown in Figure 1. As it is seen in Fig. 1 the killer pellet moves toward the central region quickly and leaves behind a cold plasma in its way. In the mixture case cooling the plasma from the edge to the central region takes much longer than in the killer pellet case. However, in these typical cases the current quench rate of both techniques is very similar. It is worth nothing that the penetration of the killer pellet was not deep into the interior region since the speed of the pellet in JT-60 was lower than that from low-field side due to the usage of a long curved tube to deliver the pellets from the high-field side. The injection speed was ~100 m/s. The current quench rate in the hydrogen case is lower than that in the other cases. Obtaining a higher current quench rate is one of the advantages of adding a small concentration of impurities in hydrogen in order to amplify the total radiation.

The benefits of injecting a mixture of impurities and hydrogen to terminate the discharges without runaway electron generation were demonstrated in ref. [3]. Now we are looking for an optimal noble gas, i.e. the one which leads to a fast energy removal as well as avoiding runaway electrons. In another set of experiments we have repeated the mixture experiments (see ref. [3]) now with measuring the heat flux to the divertor plates and also with changing the noble gas elements to compare their effects on disruption deleterious effects. The waveforms of selected plasma parameters for 3 different shots terminated by argon, krypton and xenon gases are shown in Fig. 2. Apart from the electron density and hard x-ray emissions all the waveforms are similar for the three shots. A higher electron density for lower Z impurities was observed. Hard x-ray emission is not increasing (or decreasing) with the atomic number of injected gases; the hard x-ray emission with krypton injection is the lowest compared to the argon and xenon injection cases. A summary of the generated runaway electrons and heat flux to the divertor plates for 10 different discharges is shown in Fig 3. As it is seen in Fig. 3 less runaway electrons and heat flux to divertor plates was observed in the mixture cases,

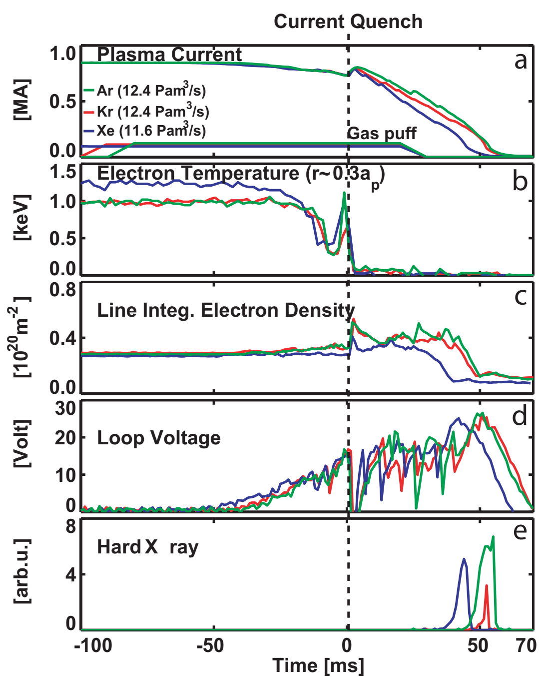

Figure 2. Plasma parameters after argon, krypton, and xenon gas puffing into ohmic plasmas. All plasma parameters have very similar time histories except for the hard X-rays. In the krypton case the level of hard x-ray signals is lowest.

particularly in those with krypton gas puffing. The details of these observations are addressed in the following subsections.

2.1.1. Runaway electron generation

An advantage of a mixture gas puffing above only impurity injection is its success in avoiding the runaway electron generation [3]. As it is seen in Fig. 3 the number of generated runaway electrons is minimal when a mixture of impurity and hydrogen gases was injected. Furthermore, lower hard X-ray emission is clearly seen in krypton cases. It is worth noting that the data were taken from discharges with almost same target plasma parameters and configuration. The plasmas were in equilibrium until sometime after runaway electron generation phase (i.e. no vertical displacement event occurred).

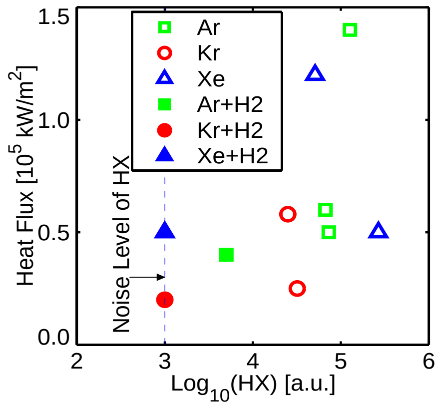

Figure 3. The summary of the heat flux and hard X-ray emissions after injecting different impurities into stable ohmic plasmas. Lower heat flux and runaway electrons are observed with mixture injections and krypton injections.

2.1.2. Modeling of runaway electron generation

To analyze the data based on the existing physics models for runaway electrons we have extracted the resistive electric field from the flux loop data (poloidal magnetic flux, Ψ_p) of a loop very close to the surface of plasma and considering Poynting's theorem, $I_pV_L=I_pV_{res}+d(0.5L_iI_p^2)/dt$. Where $L_i=\mu_0Rl_i/2$, l_i is internal inductance, $V_L=d(\Psi_p)/dt$, I_p is the plasma current, R is the major radius, V_{res} is the resistive voltage, and $E_{res}=V_{res}/2\pi R$ is the resistive electric filed. Basically, runaway electrons are generated when the normalized electric filed, $\varepsilon=E_{res}/E_c$, exceeds unity, where E_c is the critical electric field above which runaway electrons are generated and it is given by $E_c\approx 0.1n_{T,20}$ [V/m] with $n_{T,20}$ being the total electron density (free+bound) in units of 10^{20} m^{-3}. The population of the generated runaway electrons and its growth rate for small E_{res}/E_c is determined by [4]:

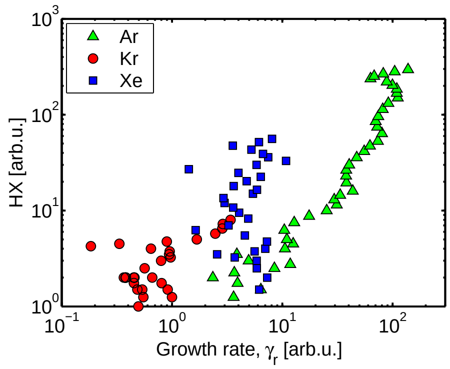

Figure 4. Hard X-ray emissions versus the growth rate of runaways for 3 different shots terminated by argon, krypton, and xenon gas puffing.

$$\gamma_r \propto \frac{1}{(\overline{Z}+1)}\frac{E_{res}}{E_c}\left(\frac{E_{res}}{E_c}-1\right). \qquad (1)$$

Here $\overline{Z}=\Sigma_i Z_i^2 n_i/\Sigma_i Z_i n_i$ is the effective charge with Z_i being the *atomic number* of different impurities in the plasma.

A summary of the calculations for 3 different experiments with different impurities (no hydrogen gas puff) are shown in Fig 4. The data were selected during the runaway electron generation phase (see Fig. 2e). The observed hard x-ray emissions increase with increasing the growth rate, γ_r. For the krypton case a lower normalized electric field was obtained compared to argon which that to a lower hard x-ray emission.

Based on equation (1) the runway electron growth rate has an inverse relation to the average charge and it has a direct relation with ε which is a function of resistive electric field and density. The resistive voltage and total electron density, n_{eT}, for discharges under consideration are plotted in Fig. 5 versus each other. The resistive electric field in the krypton case is lower than that in the xenon and argon cases and its atomic charge is somewhat between that of argon and xenon. The lower resistive electric field and high n_{eT} for krypton case might have been a reason for observing less hard X-ray emissions in this case. On the other hand, the resistive voltage in the xenon and argon cases is very similar while the effective charge in the xenon case is much higher ($\overline{Z} \sim Z$). The high effective charge in the xenon case compensates the effect of the high resistive electric field in the generation of runaway electrons. Therefore, a lower hard X-ray signal is observed in the xenon case relative to the argon case.

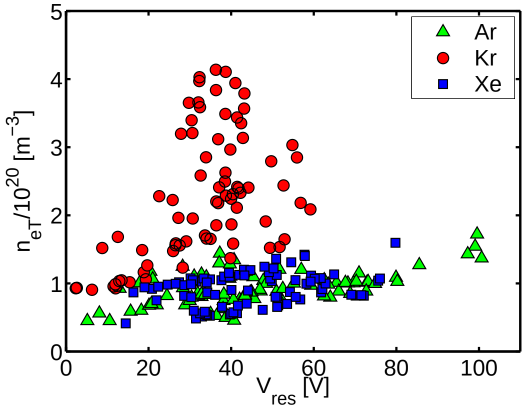

Figure 5. Total electron density versus resistive voltage for 3 different shots. Lower resistive electric field and higher electron density were evaluated during the runaway electron phase with krypton injection.

2.2. Enhanced Loss of Runaway Electrons by Impurity Pellet Injection

We consider that impurity pellet injection is a candidate as a quick actuator for mitigation of runaway electrons by increase in n_e and/or Z_{eff}. However, since electron temperature is very low as ~10 eV at a post-disruption runaway plasma [8], where most of plasma current is driven by runaway electrons, ablation rate of a pellet by bulk electrons is very low. So, we expect pellet ablation by high-energy runaway electrons themselves.

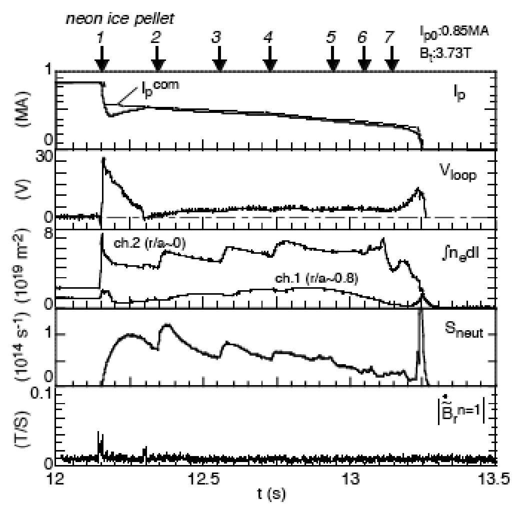

Figure 6. Waveforms of experiments for impurity pellet injection into a post-disruption runaway plasma. I_p-plasma current, V_{loop}-one turn loop voltage, $\int n_e dl$-line integrated electron density, Sneut-photo neutrons, $\left|\tilde{\dot{B}}_r^{n=1}\right|$ indicator of MHD activity of n=1 mode.

Figure 6 shows waveforms for impurity pellet injection experiment into a post-disruption runaway plasma. A series of neon ice pellets (2.1mm×2.1mm, ~700 m/s, 5 Hz, LFS) are injected into an Ohmic hydrogen discharge. The 1st pellet works as the "killer pellet" to cause intentional disruption accompanied by a runaway plasma phase with starting current of ~0.5 MA, which corresponds to ~2.3×10^{17} runaway electrons. Divertor configuration is kept until t~12.95 s, then the plasma begins to shrink with outer-touched limiter configuration. Control of plasma current is programmed as indicated by command value I_p^{com} in Fig 6.

Successive six neon ice pellets are injected for the experiment and we have observed the clear increase in line integrated electron density $\int n_e dl$ along the central chord ch.2 (r/a~0) for 2nd to 4th pellet injection. For the 2nd pellet, increment of line averaged density $\Delta\{\int nedl(r/a\sim0)/Lp\}$ of ~0.72×10^{19}m^{-3} (Lp is the chord length ~2.3 m) is ~30% of that for the 1st "killer pellet" of ~2.4×10^{19} m^{-3}. Though pellet deposition must be different for those pellets, if we assume that the neon atoms are fully ionized for the 1st pellet, i.e. Z_{Ne}=10, Z_{Ne} can be around 3 for the 2nd pellets. This is consistent with the ionization equilibrium of neon at T_e=10 eV. Also, Z_{eff} of around 3 is evaluated by visible bremsstrahlung measurement. These things suggest that the runaway plasma is nearly pure neon plasma with T_e~10 eV. Since estimated ablation time using NGS model for the neon pellet by the bulk electrons [9] is the order of 10 s, significant contribution by runaway electrons to pellet ablation shall be important. One hypothesis is that runway electrons evaporate and/or weakly ionize the pellet substance, then ionization is progressed mainly by bulk electrons to the equilibrium state. For 5th to 7th pellet injection, plasma response is not obviously seen. There, data of pellet size monitor before plasma injection indicate that the 5th pellet was broken and size of the 6th pellet was smaller. For the 7th pellet, smaller number of runaway and bulk electrons and change in plasma configuration should be considered in ablation process. Also, changes in energy and spatial distributions of runaway electrons are important factors, but there is less information about them at the present.

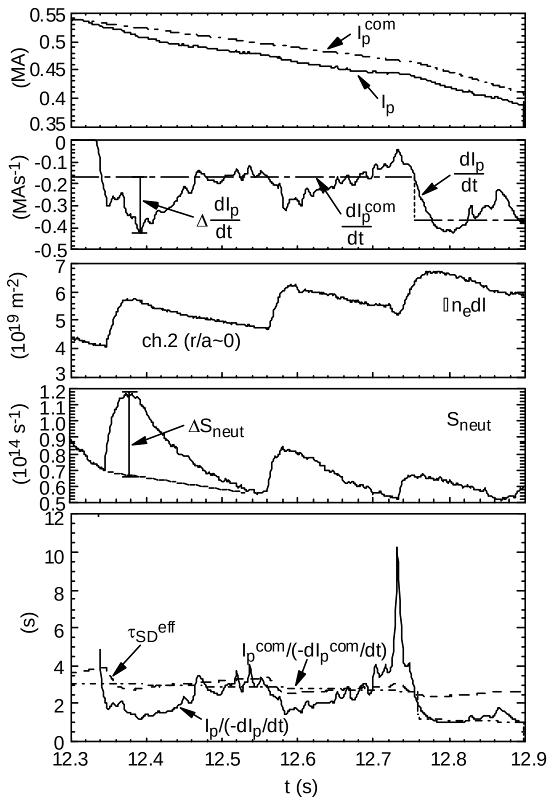

Figure 7. A detail of waveforms of experiment for impurity pellet injection into a post-disruption runaway plasma current and increase in photo-neutrons for 2nd and 4th pellet injections are confirmed. Enhanced loss of runaway electrons from plasma by impurity pellet injection is found as seen in current decay time Ip/(-dIp/dt).

For injections of 2nd to 4th pellet, increases in neutron emission rate S_{neut} are observed as shown in Figs. 6 and 7. The S_{neut} indicates photo-neutrons emitted when runaway electrons are lost and hit the wall. Threshold energies of the photo-nuclear reactions are

8-30 MeV for nickel and ~26 MeV for carbon [10], while the free-fall electron energy is calculated with loop voltage as ~20 MeV at t=12.3 s. Corresponding to S_{neut} signal, we observe the reduction of runaway plasma current I_p as seen in Fig.7. Current decay rate dIp/dt shows it very clearly. Recovery of I_p to be closed to commanded value I_p^{com} is presumably due to the knock-on generation of runaway electrons. Decay time of runaway plasma current $I_p/(-dI_p/dt)$ at pellet interval time, e.g. t~12.55 s, is ~ 3 s, which consists with command decay time. On the other hand, the decay time at pellet injection phase becomes shorter than command value for the 2nd and 3rd pellet, e.g. ~1.5 s at t~12.4 s. Estimated effective slowing down time of runaway electrons by friction with bulk plasma τ_{SD}^{eff} also decreases due to increase in density, and its tendency is similar to that of $I_p/(-dI_p/dt)$ as shown in Fig.7. But it seems not enough for full explanation of the $I_p/(-dI_p/dt)$~1.5 s. One possible mechanism to contribute such the enhanced decay at the pellet injection is scattering of runaway electrons in the pellet substance and dense pellet cloud. This scattering may resulted in increase in transport of runaway electrons and also large synchrotron radiation by increase in pitch angle [11],[12]. The decay time by synchrotron radiation of ~1.5s is estimated for 20 MeV electrons if those pitch angle is ~0.06 rad., but no direct evidence for it at the present. Since little change in MHD activities are observed at pellet injections as seen in Fig.1, contribution of MHD activities to enhancement of loss of runaway electrons seems very small.

For the period between t=12.34 s and t=12.39 s in Fig.7, reduction of I_p is about 3 kA which corresponds to the loss of ~1.5×10^{15} runaway electrons, and increment of neutron yield Y_n is ~1.5×10^{12} neutrons. Here, the ratio of Y_n per a runaway electron of ~1×10^{-3} is in good agreement to the scaling of photo-neutron yield for a 20 MeV electron [10], which indicates that loss of runaway electrons from the plasma substantially contributes the reduction of I_p. Figure 8 shows the relationship between increment of decay rate of runaway plasma current $\Delta I_p/(-dI_p/dt)$ and increment of photo-neutron signal ΔS_{neut} for 2nd to 4th pellet injection. Such almost linear relationship simply supports that larger reduction of runaway current is attributed to larger loss of runaway electrons. The reason why ΔS_{neut} is smaller for 3rd and 4th pellet injections are not clear yet, but change in energy and spatial distributions of runaway electrons should be considered, again. In order to promote loss of runaway electrons, presumably increase in pellet size, injection frequency, and atomic number will be helpful, but further investigations are needed.

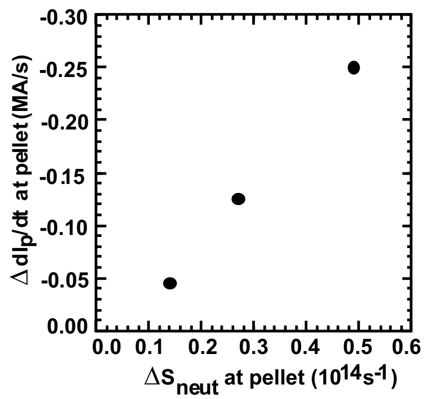

Figure 8. relationship between increments of decay rate of runaway plasma current ΔdIp/(-dIp/dt) and photo-neutrons signals ΔSneut for 2nd to 4th pellet injections.

3. Summary and conclusions

Different disruption mitigation experiments were carried out in the JT-60U with ohmic plasmas using killer pellets and noble gas puffs with and without strong hydrogen puffs.

From a comparison of discharges terminated by a killer pellet injection, hydrogen gas puffing, and mixture of hydrogen and argon gas puffing we have found that a similar current quench with killer pellet and mixture injection was obtained that was faster than the current quench that was observed with massive hydrogen gas puffing only.
Comparing different discharges terminated by puffing different noble gases, argon, krypton, and xenon with or without hydrogen gas puffing we evaluated that:

1. Low heat fluxes to the divertor tiles and low amounts of runaway electrons were generated in the noble gas and hydrogen mixture cases, in particularly those with krypton and hydrogen. The number of runaway electron generated with a xenon gas puff was smaller than that with an argon puff.
2. It was found that the resistive electric field during the current quench with a krypton puff was less than that with an argon or xenon puff.
3. A high effective charge was evaluated with a xenon puff resulting in a high bound and free electron density. Even with this higher resistive electric field the normalized electric field in xenon was less than that for argon resulting in a lower amount of runaway electron.

Experiment of impurity neon pellet injection into a post-disruption runaway plasma has been carried out to study the way to mitigate runaway electrons by an external actuator. We have found the effect of impurity pellet to enhance the loss of runaway electrons from the plasma.

Acknowledgments

On of the authors (M. B.) expresses his gratitude to Dr H. Kishimoto for his continuous encouragement and support throughout the work. Helpful suggestions by Drs. K. Tsuzuki, M. Kikuchi, M. Nagami, T. Takizuka, and S. Konoshima are gratefully acknowledged.

References

[1] YOSHINO, R., et al., Plasma Phys. Control. Fusion **39** (1997) 313.
[2] WHYTE, D.G., et al., Physical Review letters **89** (2002) 055001.
[3] BAKHTIARI, M., et al., Nuclear Fusion **42** (2002) 1197.
[4] ROSENBLUTH, M.N. et al , Nucl. Fusion **37** (1997) 1355.
[5] YOSHINO, R., et al., Nucl. Fusion **39** (1999) 151.
[6] YOSHINO, R., Tokuda, S., Nucl. Fusion **40** (2000) 1293.
[7] TAMAI, H., et al., Nucl. Fusion **42** (2002) 290.
[8] HATAE, T., et al., Rev. Sci. Instrum. **70** (1999) 772.
[9] KUTEEV, B.V., et al., Nucl. Fusion **35** (1995) 1167, and APS 1999.
[10] JARVIS, O. N., et al., Nucl. Fusion **28** (1988) 1981.
[11] GILL, R. D., Nucl Fusion **33** (1993) 1613.
[12] HELANDER, P, et al., Plasma Phys. Contr. Fusion **44** (2002) B247.